Mixed-Valence Ce/Zr Metal-Organic Frameworks: Controlling the Oxidation State of Cerium in One-Pot Synthesis Approach

Maria Ronda-Lloret, Isaac Pellicer-Carreño, Aida Grau-Atienza, Roberto Boada, Sofia Diaz-Moreno, Javier Narciso-Romero, Juan Carlos Serrano-Ruiz, Antonio Sepúlveda-Escribano, and Enrique V. Ramos-Fernandez*

The preparation of MOFs including a metal with an easily exchangeable oxidation state, while maintaining the same crystal structure and stability, is of paramount importance for myriad applications. In this work, a new synthesis method is reported that can be used to prepare Ce/Zr-MOFs (UiO-66 structure) having only Ce(III), a mixed-valence Ce(IV)/Ce(III), or only Ce(IV) cations, as desired. The materials are characterized using a large number of techniques, including X-ray absorption and X-ray photoelectron spectroscopies.

1. Introduction

The presence of metal species that can easily exchange their oxidation states is of paramount importance in the field of catalysis,[1,2] sensors,[3] photocatalysis,[4] among others. A classic example is ceria (CeO_2), in which Ce(IV) can readily be reduced to Ce(III) under an adequate environment, and vice versa. The major drawback of CeO_2 for being applied in catalysis is that only the surface of the crystallites is used in the catalytic event.[5–7] Therefore, most of the cerium and oxygen atoms of the lattice are not used. One promising alternative to better take advantage of ceria properties is the dispersion of CeO_2 nanoparticles on an inert support, as we and others have already demonstrated.[8–10] Another approach might be the construction of porous solids made of molecularly dispersed cerium oxide clusters that allows reactants to reach the clusters. In this sense, metal–organic frameworks (MOFs) may be an opportunity to prepare this type of solids, since cerium MOFs might be constructed.

Although there have been some attempts to prepare Ce-containing MOFs, their stability is limited. Stock's group and others have reported the preparation of Ce MOFs in which Ce(IV) is introduced.[1,11] The presence of the Ce(IV)/Ce(III) redox pair has been demonstrated by de Vos.[12] In this recent work, they used X-ray absorption spectroscopy (XAS) to demonstrate that Ce(III) cations could be generated using 2,2,6,6-tetramethyl-1-pi-peridinylox (TEMPO) as reductant, and that they can be re-oxidized back to Ce(IV) using oxygen as oxidant. However, the presence of the redox pair is induced during the reaction but is not present in the pristine MOF.

The main drawback of the cerium-based MOFs is their low thermal stability that limits their applications to room temperature processes. However, stability and redox behavior can be enhanced by introducing Zr cations in the same cluster, in such a way that it can be compared with ceria-zirconia mixed oxides.[1] Another important point is the tailoring of the oxidation state of the cerium cations that are present in the MOF.

Saying so, the preparation and characterization of these mixed-metal MOFs is far from being trivial, since we can find different situations such as the formation of segregated phases (differentiated Ce-MOF and Zr-MOF crystallites), clusters having only Ce or Zr in the same crystallite and, finally, the desired one, clusters containing both cations, that is, a true mixed-metal MOF.

Besides the true mixed-metal nature of the MOF, it is also crucial to control the oxidation state of Ce. Ce(III) and Ce(IV) are both stable at ambient conditions depending on the environment, and both of them have the same coordination number with carboxylic acid groups, although their ionic diameter is pretty different; thus, both can be used for producing MOFs with the same topology. The tailoring of the oxidation state of the Ce cations is expected to lead to a fine control of the redox properties.

The synthesis of Zr— and Ce-based carboxylate MOFs (UiO-type) is normally assisted by the use of modulators, which are monocarboxylic acids that are incorporated into the synthesis media and have an important role controlling the formation of the clusters ($Zr_6O_4(OH)_4$) and the crystal growth kinetics. The effect of the acid media and the amount of modulator have

M. Ronda-Lloret, I. Pellicer-Carreño, Dr. A. Grau-Atienza,
Dr. J. Narciso-Romero, Prof. A. Sepúlveda-Escribano,
Dr. E. V. Ramos-Fernandez
Laboratorio de Materiales Avanzados
Departamento de Química Inorgánica – Instituto Universitario de
Materiales de Alicante Universidad de Alicante
Apartado 99, Alicante E-03080, Spain
E-mail: enrique.ramos@ua.es
Dr. R. Boada, Dr. S. Diaz-Moreno
Diamond Light Source
Didcot, Oxfordshire OX11 0DE, UK
Dr. J. C. Serrano-Ruiz
Department of Engineering
University of Loyola
Campus Sevilla Avda. de las Universidades s/n, Dos Hermanas, Seville
41704, Spain

been studied, and it has been found that both the acidity and the chemical nature of the modulator greatly affect the crystal size and morphology.[13,14]

Modulator-assisted synthesis can also modify the chemical nature of the MOF, since the modulator molecules are attached to the cluster and remain in the final structure. De Vos et al. have demonstrated that the modulator attached to the cluster can strongly modify the electronic properties and consequently, the catalytic behavior of the MOF.[15,16] Furthermore, it has been also provided that the presence of molecules such as formic acid or dimethylamine (that might be considered as modulators) change the oxidation state of the metal during the synthesis. This happens with metals that have a high redox potential such as manganese ions that may oxidize the organic molecules.[14]

Formic acid is usually used as modulator in MOF synthesis; moreover, it is well known that formic acid can be a powerful reductant. Its redox potential is negative $E_r^0(H_2,CO_2/HCOOH)$ = −1.99 V. Actually, it is used as reducing agent in several reactions such as nitrate reduction.[17] If we take into account the redox potential of the metals involved in the MOF that we want to obtain, we can see that the redox potential of the E_r^0 (Zr(IV)/Zr(III)) = −2.5 V pair is negative, while the potential of the E_r^0 (Ce(IV)/Ce(III)) = +1.61 V pair is positive at standard conditions.[18,19] Thus, Ce(IV) has the tendency to be reduced at standard conditions, while Zr(IV) is difficult to reduce. Although the reduction potential can be modified by tuning the reaction conditions (pH, complexation, etc.), in principle we can assume that the main factor to consider is the standard reduction potential E_r^0. All the above indicates that by playing in a clever way with the cerium precursor, the amount and nature of the modulator and the synthesis conditions, we can design the formation of MOFs having Ce(III) or Ce(IV) species, as desired.

Herein, a one-pot synthesis method is reported that enables us to prepare true (Zr,Ce) mixed-metal UiO-66 with tailored redox properties. This method allows the preparation of mixed-metal MOFs having only Ce(III), Ce(IV), or even mixed valence MOFs with Ce(III)/Ce(IV). The designed synthetic method makes use of a modulator to finely control the oxidation state of the cerium cations. The local environment of the metal cluster, as well as the electronic properties, have been investigated by element selective techniques such as XAS and X-ray photoelectron spectroscopy (XPS), which have confirmed the success of our approach.

2. Results and Discussion

For the first attempt to prepare UiO-66(Zr,Ce) mixed metal MOF having exclusively Ce(III) cations, we followed the approach reported by Bandosz et al.[20] In this approach, they used a one-pot, modulator-free synthesis in which stoichiometric amounts of ZrCl$_4$ and CeCl$_3$·7H$_2$O were used as metal precursors. These authors analyzed the presence of Ce(III) in their sample by infrared spectroscopy, and one of the vibrational modes they observed was ascribed to Ce(III) coordinated to the carboxylic group. However, no information was reported on the presence of Ce(IV). Furthermore, the presence of Ce(III) does not fully prove the formation of the true mixed metal
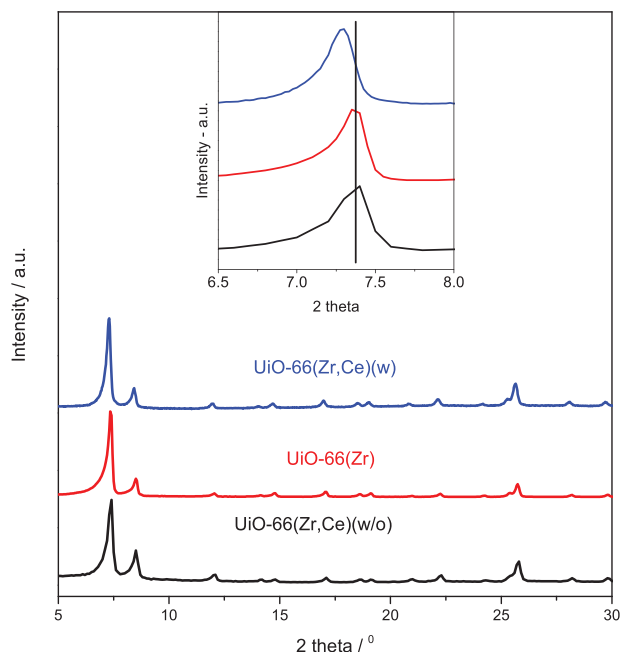

Figure 1. X-ray diffraction pattern of samples UiO-66(Zr) (red), UiO-66(Zr,Ce)(without) (black), and UiO-66(Zr,Ce)(with) (blue).

UiO-66(Zr,Ce) material. Following this approach (see Experimental Section for details), we synthetized the sample named UiO-66(Zr,Ce)(without), following the labeling used by as Bandosz.[20] The notation (without) indicates that the synthesis was done without modulator. We have also prepared a sample in which we used a similar approach but with formic acid as modulator. The obtained sample was labelled as UiO-66(Zr,Ce) (with).

Figure 1 shows the X-ray diffraction patterns of the samples prepared. The samples have been compared against a commercial UiO-66(Zr) material supplied by Strem.

As we can see, the XRD patterns look very similar, indicating that the UiO-66 structure has been successfully obtained for all the samples. The only remarkable feature that can be observed (see inset in Figure 1) is that the main diffraction peak of UiO-66, the (1,1,1) reflection at 2theta ≈7.4°, is shifted towards lower angles for the sample prepared with formic acid, indicating that there is a change in the unit cell of the framework. This suggests that some cerium cations get incorporated in the framework, but it is not an evidence of the incorporation of cerium cations into the MOF cluster. Furthermore, we have no information about the oxidation state of the cerium cations.

In order to assess the effect of the modulator in the textural properties of the prepared materials we have also measured the N$_2$ adsorption isotherms, which are plotted in **Figure 2**. In both cases type I isotherms are obtained,[21] which are characteristic of microporous solids. The main difference between both samples is that the one prepared without a modulator has a less accessible surface area, pointing to a lower amount of accessible porosity. It has been reported that the nucleation of UiO-66 without using a modulator is fast, and it generates agglomerates and small amounts of amorphous (non-porous) material.[22–24] A sample UiO-66(Zr,Ce)(with) has a higher surface
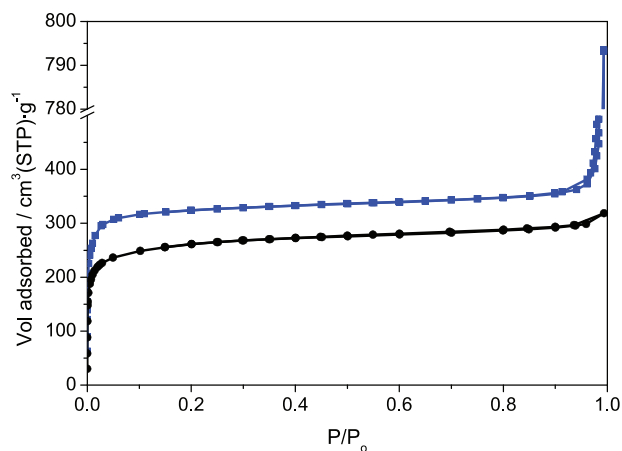
Figure 2. N₂ adsorption isotherms of the following samples, UiO-66(Zr,Ce)(without) (black) and UiO-66(Zr,Ce)(with) (blue).

area, what proves that that the modulator has a structural effect. We have also measured thermal stability by thermogravimetric analysis and have found that the absence of a modulator changes the stability and also the amount of residual inorganic matter. The results are shown in Figure S1, Supporting Information. As can be seen, the modulator produces a more stable sample. This higher stability together with the lower amount of residues that remain after the TGA experiment indicates that the sample is more crystalline and that the linkers are forming part of the structure and not occluded in the porosity and this is the reason why the UiO-66(Zr, Ce)(with) has a higher surface area.[25] After the synthesis, the materials were analyzed by inductively coupled plasma (ICP). We found that, for both samples, we could only incorporate 4 wt% of cerium cations, even though we used 1:1 Zr:Ce ratio in the synthesis mixture. Thus, not all the cerium added to the synthesis mixture was incorporated in the UiO-66 structure. The fact that we used a Ce(III) precursor in the synthesis of the MOF may be the reason, since its ionic diameter is different than that of Zr(IV), thus limiting the number of Ce cations that might be incorporated.

To check if the cerium cations have been incorporated into the MOF's cluster forming a true mixed-metal UiO-66, the samples were analyzed by different X-ray techniques: XPS, X-ray absorption near edge structure (XANES) and extended X-ray absorption fine structure (EXAFS). While XPS and XANES provide information on the oxidation state of the elements present in the samples, EXAFS provides information local structural information around the atom probe. Thus, the combination of these techniques will shed light on both the chemical and the structural nature of the metal clusters in the prepared samples.

First, Zr was analyzed by XPS. Figure S2, Supporting Information, shows the XPS spectra of the Zr 3*d* core level. The spectra of the different samples show the well-resolved spin-orbit component of this level and, as it can be seen, there are not significant differences in the spectra. We have also analyzed the O 1*s* (see Figure S2, Supporting Information) core levels and we have not found significant changes. This is due to two factors. First, the amount of cerium incorporated is rather small; second, the XPS is sensitive to changes in oxidation states and, in this case, the incorporation of cerium will not modify the

electronics of the system to a great extent. Some authors have found significant changes in the Zr 3*d* core level of the samples when incorporating a second metal in the cluster, for example Ti, but the changes were only detected when there was a larger amount of Ti than Zr in the cluster.[26] This points to the difficulty to see changes in the Zr 3*d* core level just by incorporating a second metal in the UiO-66 structure.

In order to assess the structural changes induced in the cluster upon incorporation of Ce, XAS measurements at the Zr K-edge were performed at the I20-Scanning beamline of Diamond Light Source.[27–29] Prior to the measurements, the samples were activated "in situ" by heating them at 150 °C for 2 h under dynamic vacuum in order to remove the adsorbed molecules that greatly affect the EXAFS spectrum of the UiO-66, as shown by Valenzano and coworkers.[30] However, we found that the activation was not fully achieved. **Figure 3** shows the XAS results. The top panel displays the XANES region of the spectra for the three samples. When cerium is incorporated in the structure, there is a noticeable decrease in the intensity of the white-line (first resonance after the edge) respect to UiO-66(Zr). The decrease of the white-line intensity can be associated with a change in the local environment around Zr related with the distortion of the Zr—Zr distances when Ce substitutes Zr in the cluster. The distortion of the cluster is also supported by the trend observed when comparing the extracted EXAFS signals (mid panel). The amplitude of the oscillations decreases with the incorporation of the cerium cations, being larger when the modulator is added to the synthesis, UiO-66(Zr,Ce)(with). This clearly indicates that cerium cations are incorporated in the same cluster as that of Zr distorting the local environment around the Zr cations.

A better understanding of the distortion is obtained when representing the pseudo-radial distribution function obtained from the Fourier transform of the EXAFS signal (bottom panel). Three shell contributions can be identified in the R-space (not phase shift corrected). The first peak, centered at 1.55 Å, can be associated to the Zr—O_a distance of the bridging oxygen (2.12 Å[30]) of the clusters. The second one, centered at 1.81 Å, can be assigned to the Zr—O_b distance of the Zr atoms bound to the carboxylate ligand (2.27 Å[30]) (see **Scheme 1**). The comparison reveals that the intensity of the Zr—O_b shell decreases with the incorporation of the cerium cations, indicating that the formation of the true mixed metal MOF produces a loss of linkers (defects).

The third peak, centered at 3.15 Å, can be ascribed to the Zr—Zr distance (3.53 Å[30]). This contribution drastically decreases when Ce is incorporated into the framework. The obtained results indicate that our synthesis provides clusters that are composed by Zr and Ce cations in close proximity.

The cerium precursor used in the synthesis was Ce(III), but the final oxidation state of the cerium cations in the MOF is, a priori, not known. In order to get a further insight, XANES measurements at the Ce L₃-edge and XPS following the electron emitted from the Ce3*d* core level were performed.

The XPS Ce 3*d* spectra is rather complex (see **Figure 4**), and it can be deconvoluted in multiple peaks. The description and assignment of the different multiplets and satellites has been deeply studied in the literature.[31–33] For example, the Ce 3*d* spectrum from a pure CeO₂ sample will have six

**ADVANCED
SCIENCE NEWS**
www.advancedsciencenews.com

**ADVANCED
FUNCTIONAL
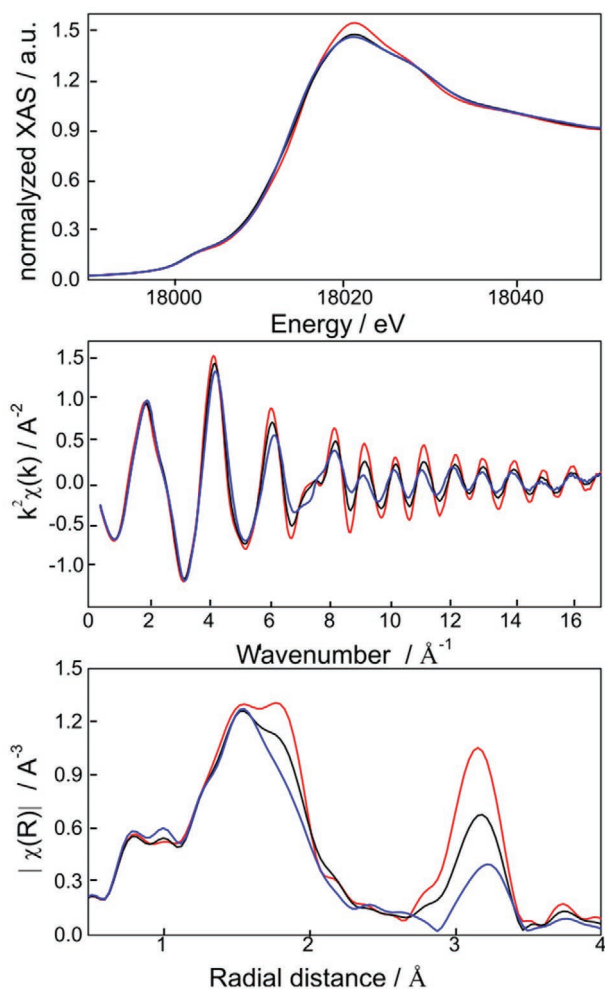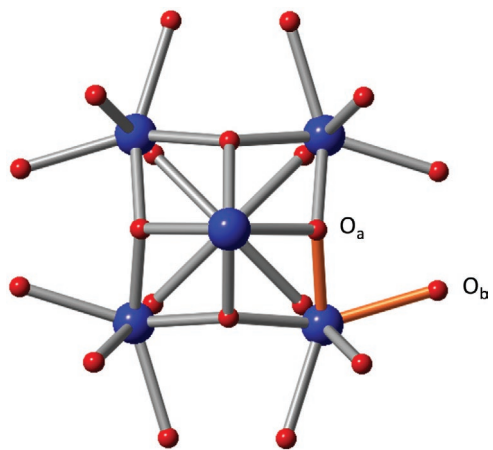MATERIALS**
www.afm-journal.de

Figure 3. X-ray absorption spectroscopy measurements at Zr K-edge. Top panel, XANES region; mid panel, EXAFS region; and bottom panel, module of the Fourier transform of the EXAFS signal. UiO-66(Zr) (red), UiO-66(Zr,Ce)(without) (black), and UiO-66(Zr,Ce)(with) (blue).

Scheme 1. Representation of the UiO-66 cluster. The type of oxygen that the cluster contains is also indicated.

visible components, even though there is only one chemical state. There is only one feature that distinguishes Ce(IV) from Ce(III) in the Ce $3d$ spectrum, and it is the satellite peak located at 916.8 eV that is characteristic of Ce(IV). This satellite peak is far enough from the Ce(III) peaks and does not overlap with them. The main difference between UiO-66(Zr,Ce)(without) and UiO-66(Zr,Ce)(with) is the satellite peak characteristic of Ce (IV) which is present in the sample prepared without modulator, indicating that during the synthesis of the MOF part of the Ce(III) is oxidized to Ce(IV). On the other hand, the presence of Ce(IV) is not detected when formic acid is used as modulator. It has been mentioned above that the presence of a powerful reducing agent, as formic acid, can control the oxidation state of the metal. In this synthesis, formic acid avoids the oxidation of Ce(III) to Ce(IV). This is, it can control the final oxidation state of the Ce cations in the framework. Hence, formic acid is acting as a double modulator on the structure and the chemical state of Ce. This result suggests that UiO-66(Zr,Ce)(with) is exclusively formed with Ce(III) cations; however, the XPS measurements on UiO-66(Zr,Ce)(without) do not allow us to discern the proportion Ce(IV):Ce(III) cations, since the peaks assigned to both oxidation states overlap in the same region.

To check this point, we measured the Ce L$_3$-edge XANES spectra. The spectra of the two MOFs, together with two references, CeO$_2$ (Ce(IV)) and Ce(NO$_3$)$_3$·6H$_2$O (Ce(III)), are represented in Figure 4. We can see that the spectra of UiO-66(Zr,Ce) (with) only shows a main feature centered at 5723 eV. Comparing this spectrum profile with the one of the Ce(NO$_3$)$_3$·6H$_2$O we can undoubtedly ascribe this resonance to Ce(III). UiO-66(Zr,Ce)(without) spectrum shows three main features, one at low energy (5723 eV) that is ascribed to Ce(III), and two more at higher energies that are characteristic of Ce(IV), as shown in CeO$_2$. This indicates that the sample contains a mixture of Ce(III) and Ce(IV) cations, suggesting that the Ce(III) cations used in the synthesis mixture were partially oxidized to Ce(IV). These results are in line with those obtained from the XPS analysis. According to our linear combination fitting analysis of the XANES spectrum using the reference compounds mentioned above, 50% of the Ce atoms are oxidized to Ce(IV).

To get a better understanding of the distortion in the cluster when Ce substitutes Zr, the Zr K-edge EXAFS signals were fitted using the Artemis program from the Demeter software package.[34] The fitting model was done considering that the concentration of Ce in the mixed (Ce,Zr) samples is 4 wt%, as determined by ICP-MS analysis. Thus, the stoichiometry is Zr$_{5.54}$Ce$_{0.46}$O$_{32}$H$_{28}$C$_{48}$. This is equivalent to ≈7.6 at% Ce substitution. Taking the approach used by Lomachenko,[35] for Ce loadings below 17 at% there are only two types of clusters, Zr$_6$ and Zr$_5$Ce. In our case, this is equivalent to have an abundance of 46% Zr$_5$Ce and 54% Zr$_6$ clusters. In other words, there is ≈1 Ce atom each 2 clusters. For our fitting model, the scattering paths related with the Zr$_6$ cluster were generated from the UiO-66 structure reported by Valenzano et al.,[30] whereas, for the Zr$_5$Ce clusters, Ce atoms were substituted in the structure considering a Zr−Ce distance equal to 3.653 Å.[35] In both clusters, Zr−O$_a$ and Zr−O$_b$ distances were left as in the original UiO-66 structure[30] and refined together for all the clusters types and for all the samples.
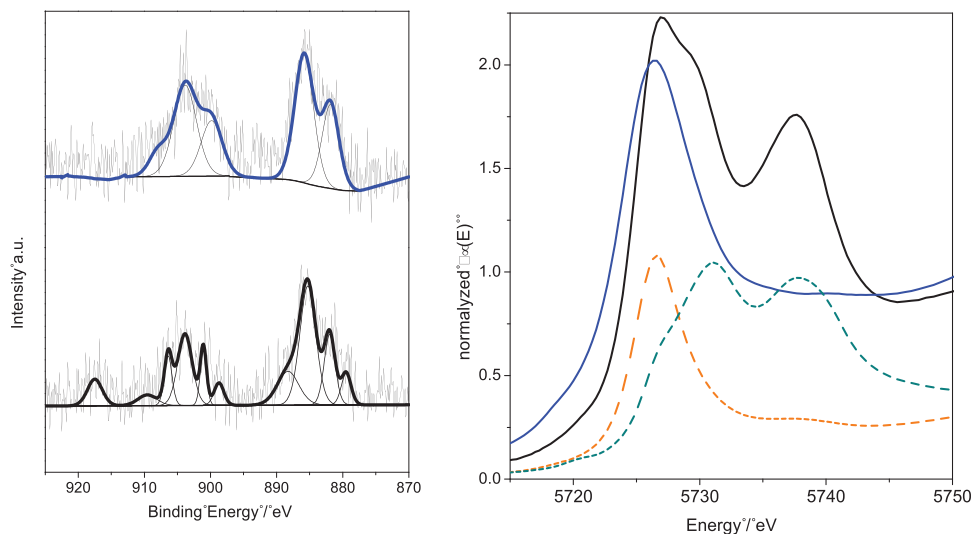
Figure 4. Analysis of the cerium cations in the different samples The right graph plots the XANES region of the Ce L3-edge transition, the right graph plots the Ce 3d level in the XPS spectra UiO-66(Zr,Ce)(with) (blue), UiO-66(Zr,Ce)(without) (black), CeO_2 (dotted green line), and $Ce(NO_3)_3 \cdot 6H_2O$ (dotted orange line).

Regarding the Zr—Zr(Ce) coordination, in the Zr_6 clusters, all the Zr atoms have 4 Zr neighbors. On the other side, for the Zr_5Ce clusters, only 1 of the 5 Zr atoms in the cluster has 4 Zr neighbors. The other 4 Zr atoms in Zr_5Ce have 1 Ce and 3 Zr atoms as neighbors.

Since our analysis of the Ce L_3-edge XANES measurements revealed that the two UiO-66(Zr,Ce) mixed metal samples have different amount of Ce(III), ≈50% Ce(III) in UiO-66(Zr,Ce) (without) and ≈100% Ce(III) in UiO-66(Zr,Ce)(with), two different Zr_5Ce clusters, $Zr_5Ce(IV)$ and $Zr_5Ce(III)$, therefore two different contributions, Zr—Ce(IV) and Zr—Ce(III) have been considered in the model. In addition, we have considered that each Ce(III) atom induces vacancies of carboxylate linkers to account for the decrease of the Zr—O_b contribution as the Ce(III) content increases as mentioned above. However, it is likely that, to keep the eightfold coordination of the Zr(IV) atoms, an —OH ligand would occupy the place of the missing linker (as we mention before the sample was not fully activated). We have also taken this into account in our model adding a Zr—OH path contribution at 2.15 Å[34] for each missing ligand.

The refinement was performed in the three samples simultaneously using the same amplitude reduction factor, S_0^2, and the ΔE as obtained in the initial refinement of the UiO-66(Zr) sample for which the structure is known.[30] The results of this preliminary fit are shown in Figures S3 and S4 and Table S1, Supporting Information. **Figure 5** shows the results obtained from the best fit. As it can be seen, the simulated spectra perfectly match the experimental one which indicates that our model and assumptions are realistic. In addition, our results are in agreement with those previously reported.[30,35] **Table 1** shows the fitting parameters including coordination number (N), interatomic distances (R), and mean-square relative displacements (σ^2, aka EXAFS Debye–Waller factors) for the different paths considered. These results confirm that the substitution of Ce(III) in the cluster induces vacancies of the carboxylate ligands (2 ligands per each Ce(III) atom) and

distorts the Zr_5Ce cluster. Upon Ce substitution, the EXAFS Debye–Waller factors for Zr—Zr and Zr—O_b contributions increase, and there is an elongation of the Zr—Zr distances to
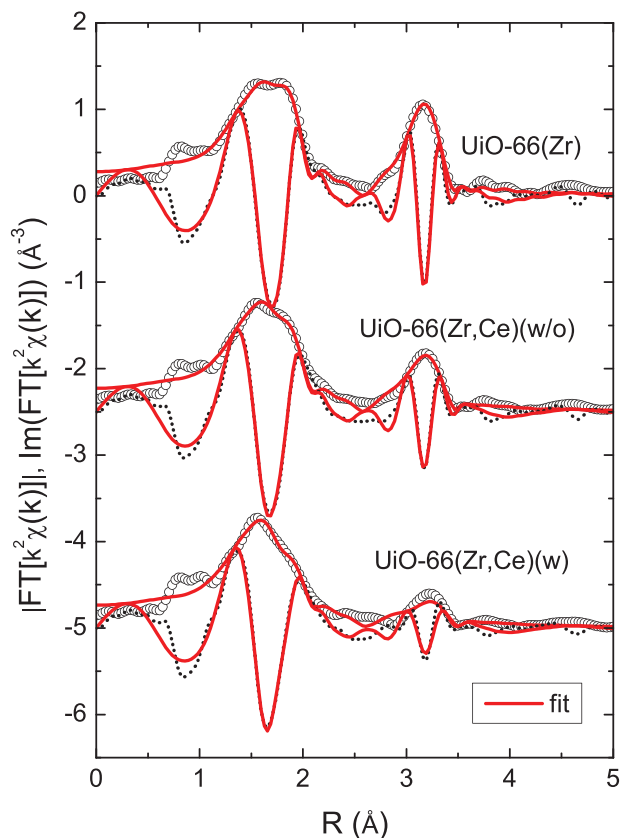

Figure 5. k^2-weighted, not phase shift corrected, Fourier transform of the Zr K-edge EXAFS signal: module (black open symbols) and imaginary part (black dotted line). The fits are represented by a red continuous line.

Table 1. Results from the EXAFS refinement of the UiO-66 samples. For the fittings, k-range: 2.54–17.3 Å^{-1}, R-range:1.1–3.6 Å^{-1}, $S_0^2 = 1.2$, and $\Delta E = 1.1$ eV. R-factor = 0.003.

	UiO-66(Zr)	UiO-66(Zr,Ce)(without)	UiO-66(Zr,Ce)(with)
N_{Oa}		2	
R_{Oa}		2.085 +/− 0.017	
σ_{Oa}^2		0.004 +/− 0.002	
N_{Ob}	6	5.76 +/− 0.13	5.54 +/− 0.12
R_{Ob}		2.246 +/− 0.008	
σ_{Ob}^2	0.005 +/− 0.001	0.006 +/− 0.001	0.008 +/− 0.001
N_{OH}		0.24	0.46
R_{OH}		2.129 +/− 0.042	
σ_{OH}^2		0.004 +/− 0.002	
N_{Zr}	4	3.63	3.63
R_{Zr}	3.525 +/− 0.006	3.526 +/− 0.007	3.543 +/− 0.013
σ_{Zr}^2	0.0049 +/− 0.0005	0.0069 +/− 0.0008	0.0116 +/− 0.0015
N_{Ce4}		0.185	
R_{Ce4}		3.638 +/− 0.100	
σ_{Ce4}^2		0.0049 +/− 0.0005	
N_{Ce3}		0.185	0.370
R_{Ce3}		3.683 +/− 0.052	
σ_{Ce3}^2		0.0058 +/− 0.0015	

Figure 6. Ce L3 XANES spectra of Pt/UiO-66(Zr,Ce)(with)(s) (blue) and UiO-66(Zr,Ce)(with)(s) (orange).

accommodate the Ce(III) atoms in the Zr$_5$Ce(III) cluster. As expected, the Zr−Ce(III) distance is larger than the Zr−Ce(IV) to account for the different ionic diameter. These results further demonstrate the success of our synthetic approach to obtain truly mixed-metal clusters.

With these experiments, it has been proved that the utilization of the modulator is essential to control the oxidation state of the second metal in the cluster. In the presented cases, we started with a Ce(III) precursor that tends to be oxidized. We wondered if we might obtain a similar result when using a Ce(IV) precursor. In order to answer this question, we have followed the approach of the Stock's group,[1,2,11] in which they used ammonium Ce(IV) nitrate, $(NH_4)_2Ce(NO_3)_6$, as the cerium precursor and a large excess of formic acid; the obtained sample was named UiO-66(Zr,Ce)(with)(s). If our approach is correct, part of the cerium cations incorporated in the framework must be in Ce(III) form. We have measured and analyzed this sample (**Figure 6**) and we have found that most of the cerium cations are incorporated as Ce(IV). This indicates that the modulator cannot reduce the Ce(IV) cations during the synthesis. This may be due to the fact that the kinetics of MOF crystallization is faster that the reduction of Ce(IV) with formic acid, this favoring the incorporation of Ce(IV) instead of Ce(III).

One way to increase the kinetics of Ce(IV) reduction is to use a catalyst in the synthesis mixture that facilitates the reaction. It is well known that noble metals favor the decomposition of formic acid generating H2, that can be dissociatively adsorbed in the noble metal and acts as a more powerful reducing agent.[36] For that reason, we decided to add to the synthesis mixture a suspension of Pt nanoparticles with mean diameter of 2 nm: Pt/UiO-66(Zr,Ce)(with)(s) (see experimental
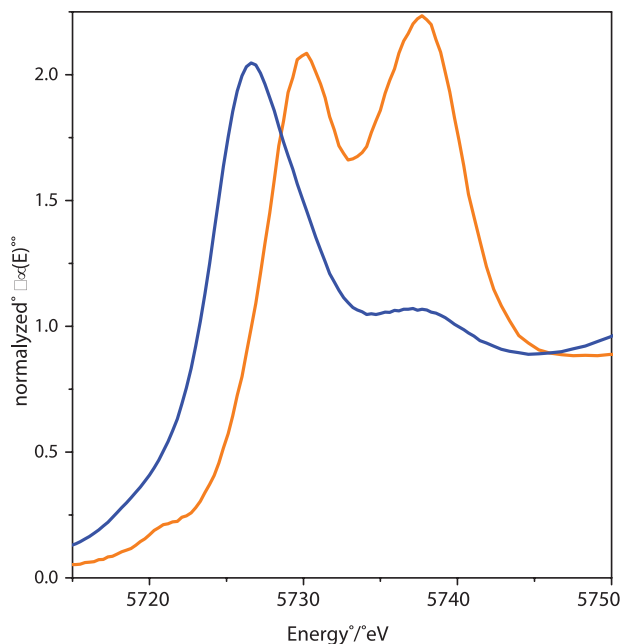
details at Supporting Information). These Pt nanoparticles will favor the decomposition of formic acid and the subsequent reduction of Ce(IV). (see XRD results in Figure S5, Supporting Information).

The XANES of this sample prepared with the addition of Pt nanoparticles presents a single white-line peak centered at 5723 eV which is characteristic of Ce(III), see Figure 6. This means that Ce(IV) was fully reduced to Ce(III) and incorporated to the framework. This result demonstrates that, with the help of the modulator (formic acid) and a small amount of promoter (Pt nanoparticles), we can incorporate the Ce(III) cations in the framework even starting with a Ce(IV) precursor.

3. Conclusion

We have found a synthetic route to prepare true-mixed metal MOF, in which we make use of a modulator, not only to modulate the crystal morphology but also the chemical nature of the metal cations. Thus, by using the modulator appropriately, we can prepare samples having only Ce(III), Ce(III)/Ce(IV), or Ce(IV) cations. We have demonstrated these facts using advanced methods such as X-ray absorption and X-ray photoemission spectroscopies.

4. Experimental Section

Experimental Details are included in the Supporting Information.

Supporting Information

Supporting Information is available from the Wiley Online Library or from the author.

Conflict of Interest

The authors declare no conflict of interest.

Data Availability Statement

The data that support the findings of this study are available from the corresponding author upon reasonable request.

[1] M. Lammert, C. Glißmann, N. Stock, *Dalton Trans.* **2017**, *46*, 2425.

[2] M. Lammert, M. T. Wharmby, S. Smolders, B. Bueken, A. Lieb, K. A. Lomachenko, D. De Vos, N. Stock, *Chem. Commun.* **2015**, *51*, 12578.

[3] L. V. Meyer, F. Schönfeld, A. Zurawski, M. Mai, C. Feldmann, K. Müller-Buschbaum, *Dalton Trans.* **2015**, *44*, 4070.

[4] X. P. Wu, L. Gagliardi, D. G. Truhlar, *J. Am. Chem. Soc.* **2018**, *140*, 7904.

[5] M. Vicario, J. Llorca, M. Boaro, C. de Leitenburg, A. Trovarelli, *J. Rare Earths* **2009**, *27*, 196.

[6] E. V. Ramos-Fernandez, N. R. Shiju, G. Rothenberg, *RSC Adv.* **2014**, *4*, 16456.

[7] W. C. Chueh, C. Falter, M. Abbott, D. Scipio, P. Furler, S. M. Haile, A. Steinfeld, *Science* **2010**, *330*, 1797.

[8] A. Gonçalves, J. Silvestre-Albero, E. V. Ramos-Fernández, J. C. Serrano-Ruiz, J. J. M. Órfão, A. Sepúlveda-Escribano, M. F. R. Pereira, *Appl. Catal., B* **2012**, *113*, 308.

[9] Y. Cao, L. Zhao, T. Gutmann, Y. Xu, L. Dong, G. Buntkowsky, F. Gao, *J. Phys. Chem. C* **2018**, *122*, 20402.

[10] J. An, Y. Wang, Z. Zhang, Z. Zhao, J. Zhang, F. Wang, *Angew. Chem., Int. Ed.* **2018**, *57*, 12308.

[11] M. Lammert, H. Reinsch, C. A. Murray, M. T. Wharmby, H. Terraschke, N. Stock, *Dalton Trans.* **2016**, *45*, 18822.

[12] S. Smolders, C. Atzori, C. Lamberti, A. L. Bugaev, D. E. De Vos, A. Struyf, N. Stock, K. A. Lomachenko, M. B. J. Roeffaers, B. Bueken, *ChemPhysChem* **2017**, *19*, 373.

[13] Z. Hu, I. Castano, S. Wang, Y. Wang, Y. Peng, Y. Qian, C. Chi, X. Wang, D. Zhao, *Cryst. Growth Des.* **2016**, *16*, 2295.

[14] M. Bosch, X. Sun, S. Yuan, Y.-P. Chen, Q. Wang, X. Wang, H.-C. Zhou, *Eur. J. Inorg. Chem.* **2016**, *2016*, 4368.

[15] F. Vermoortele, M. Vandichel, B. Van De Voorde, R. Ameloot, M. Waroquier, V. Van Speybroeck, D. E. De Vos, *Angew. Chem., Int. Ed.* **2012**, *51*, 4887.

[16] F. Vermoortele, B. Bueken, G. Le Bars, B. Van De Voorde, M. Vandichel, K. Houthoofd, A. Vimont, M. Daturi, M. Waroquier, V. Van Speybroeck, C. Kirschhock, D. E. De Vos, *J. Am. Chem. Soc.* **2013**, *135*, 11465.

[17] A. Garron, F. Epron, *Water Res.* **2005**, *39*, 3073.

[18] D. F. Shriver, M. T. Weller, T. Overton, J. Rourke, F. A. Armstrong, in *Inorganic chemistry*, 6th ed., W.H. Freeman and Company, New York **2006**.

[19] S. Ghosh, S. Vandarkuzhali, P. Venkatesh, G. Seenivasan, T. Subramanian, B. Prabhakara Reddy, K. Nagarajan, *J. Electroanal. Chem.* **2009**, *627*, 15.

[20] A. M. Ebrahim, T. J. Bandosz, *ACS Appl. Mater. Interfaces* **2013**, *5*, 10565.

[21] M. Thommes, K. Kaneko, A. V. Neimark, J. P. Olivier, F. Rodriguez-Reinoso, J. Rouquerol, K. S. W. Sing, *Pure Appl. Chem.* **2015**, *87*, 1051.

[22] M. R. DeStefano, T. Islamoglu, S. J. Garibay, J. T. Hupp, O. K. Farha, *Chem. Mater.* **2017**, *29*, 1357.

[23] B. Van de Voorde, I. Stassen, B. Bueken, F. Vermoortele, D. De Vos, R. Ameloot, J.-C. Tan, T. D. Bennett, *J. Mater. Chem. A* **2015**, *3*, 1737.

[24] E. V. V. Ramos-Fernández, J. Ruiz-Martínez, J. C. C. Serrano-Ruiz, J. Silvestre-Albero, A. Sepúlveda-Escribano, F. Rodríguez-Reinoso, *Appl. Catal., A* **2011**, *402*, 50.

[25] S. Gökpinar, T. Diment, C. Janiak, *Dalton Trans.* **2017**, *46*, 9895.

[26] A. Wang, Y. Zhou, Z. Wang, M. Chen, L. Sun, X. Liu, *RSC Adv.* **2016**, *6*, 3671.

[27] S. Hayama, G. Duller, J. P. Sutter, M. Amboage, R. Boada, A. Freeman, L. Keenan, B. Nutter, L. Cahill, P. Leicester, B. Kemp, N. Rubies, S. Diaz-Moreno, *J. Synchrotron Radiat.* **2018**, *25*, 1556.

[28] S. Diaz-Moreno, M. Amboage, M. Basham, R. Boada, N. E. Bricknell, G. Cibin, T. M. Cobb, J. Filik, A. Freeman, K. Geraki, D. Gianolio, S. Hayama, K. Ignatyev, L. Keenan, I. Mikulska, J. F. W. Mosselmans, J. J. Mudd, S. A. Parry, *J. Synchrotron Radiat.* **2018**, *25*, 998.

[29] S. Diaz-Moreno, S. Hayama, M. Amboage, A. Freeman, J. Sutter, G. Duller, *J. Phys.: Conf. Ser.* **2009**, *190*, 012038.

[30] L. Valenzano, B. Civalleri, S. Chavan, S. Bordiga, M. H. Nilsen, S. Jakobsen, K. P. Lillerud, C. Lamberti, *Chem. Mater.* **2011**, *23*, 1700.

[31] E. Bêche, P. Charvin, D. Perarnau, S. Abanades, G. Flamant, *Surf. Interface Anal.* **2008**, *40*, 264.

[32] S. Tsunekawa, T. Fukuda, A. Kasuya, *Surf. Sci.* **2000**, *457*, L437.

[33] S. Rico-Francés, E. O. Jardim, T. A. Wezendonk, F. Kapteijn, J. Gascon, A. Sepúlveda-Escribano, E. V. Ramos-Fernandez, T. A. Wezendonk, A. Sepúlveda-Escribano, E. O. Jardim, S. Rico-Francés, J. Gascon, *Appl. Catal., B* **2015**, *180*, 169.

[34] H. Fukui, M. Fujimoto, Y. Akahama, A. Sano-Furukawa, T. Hattori, *Acta Crystallogr., Sect. B: Struct. Sci., Cryst. Eng. Mater.* **2019**, *75*, 742.

[35] K. A. Lomachenko, J. Jacobsen, A. L. Bugaev, C. Atzori, F. Bonino, S. Bordiga, N. Stock, C. Lamberti, *J. Am. Chem. Soc.* **2018**, *140*, 17379.

[36] Z. Li, Q. Xu, *Acc. Chem. Res.* **2017**, *50*, 1449.